Proc. VI Int. Conf. Borate Glasses, Himeji, Japan, 18–22 August 2008 Phys. Chem. Glasses: Eur. J. Glass Sci. Technol. B, October 2009, **50** (5), 301–304

Molecular orbital calculation of the ^{29}Si NMR chemical shift in borosilicates: the effect of boron coordination to SiO_4 units

T. Nanba,[1] *Y. Asano, Y. Benino*

Graduate School of Environmental Science, Okayama University, 3-1-1, Tsushima-Naka, Okayama 700-8530, Japan

S. Sakida

Environmental Management Center, Okayama University, 3-1-1, Tsushima-Naka, Okayama 700-8530, Japan

Y. Miura

University of Shiga Prefecture, 2500, Hassaka-Cho, Hikone-City, Shiga 522-8533, Japan

Manuscript received 1 September 2008
Revised version received 28 February 2009
Accepted 15 September 2009

Borosilicate cluster models were constructed, and the ^{29}Si NMR chemical shift was estimated by molecular orbital calculations. For Q^4 species (an SiO_4 unit consisting of four bridging oxygen atoms), a higher frequency shift was confirmed due to the replacement of the surrounding SiO_4 with BO_4 units, and for Q^4 species associated with more than one BO_4 unit, the chemical shifts were nearly identical to those for Q^3 species (an SiO_4 unit including one nonbridging oxygen) in alkali silicates. The chemical shifts of Q^4 species in borosilicates were interpreted in terms of the change in bond angle of Si–O–(Si,B4) bridges. A change in chemical shift anisotropy of Q^4 species was also found. The Q^4 species associated with two BO_4 units indicated an anisotropy maximum, which was smaller than the anisotropy of Q^3 species.

Borosilicate glasses have high thermal shock resistance and high chemical durability, and hence they have been used as laboratory and heat resistant glasses. Recently, they have also been used in glass solidification of nuclear wastes. Borosilicate glasses are also known for phase separation, and they have been used as separation membranes, catalyst supports and an alternative to SiO_2 (Vycor®) glass. Structural studies have been extensively performed by various experimental techniques, such as ^{11}B and ^{29}Si NMR, XPS, IR and Raman spectroscopies, and structural models have also been proposed.(1–4) Among the models, a model proposed by Dell *et al*(1) has been commonly accepted.

Nanba *et al*(5,6) found a disagreement between the amounts of nonbridging oxygen (NBO) estimated from ^{11}B and ^{29}Si NMR analyses for borosilicate glasses with low alkali content; ^{11}B NMR suggested that all alkali ions were associated with BO_4 units as a charge compensator with no NBOs in the low alkali glasses, but ^{29}Si NMR suggested the presence of Q^3 species (SiO_4 units including one NBO) in a measureable amount. In the ^{29}Si MAS (magic angle spinning) NMR spectrum of $0{\cdot}2Na_2O.B_2O_3.0{\cdot}5SiO_2$ glass,(6) an NMR peak was successfully extracted at −90 ppm. According to a conventional peak assignment for alkali binary silicate glasses,(7) the −90 ppm peak is assigned to Q^3 species. In aluminosilicates, the ^{29}Si NMR signal shifts to the higher frequency side (lower magnetic field side) as the number of AlO_4 units surrounding an SiO_4 unit increases, and Q^4 species associated with three AlO_4 units appear as a peak at around −90 ppm in ^{29}Si NMR.(8) It was hence considered that the conventional assignments were not applicable to alkali borosilicate glasses, and Nanba *et al*(6) proposed an interpretation of the −90 ppm component in the ^{29}Si NMR spectra of borosilicates;(6) according to their molecular orbital (MO) calculations, Si2p and O1s orbital energies of Si and O atoms in B4–O–Si bridges (where B4 indicates four-fold coordinated boron) with small bond angle (~125°) were close to those of Si and O atoms in Q^3 species and NBOs in alkali silicates. It was finally proposed that in borosilicate glasses, Si atoms in such B4–O–Si bridges appeared in the −90 ppm component of the ^{29}Si NMR spectra.

In the present study, various structural models were constructed changing the number of BO_m units surrounding an SiO_4 unit, and the ^{29}Si NMR chemical shift of the Si atom in the central SiO_4 unit was calculated by using MO calculations to investigate the effect of boron coordination to SiO_4 units.

Computational

Cluster models were constructed by two methods. In the first method, the objective structural units were extracted from various crystals. In the second method, the objective structures were initially hand built, and geometrical optimisations were finally performed by using the Gaussian03 program(9) to

---

[1] Corresponding author. Email tokuro_n@cc.okayama-u.ac.jp

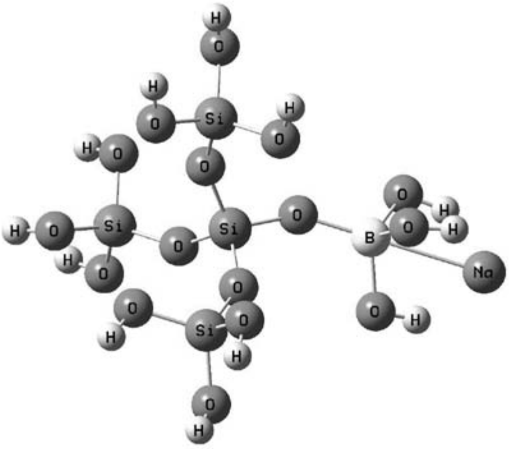

Figure 1. A cluster model of a Q^4 species surrounded by three SiO_4 units and one BO_4 unit

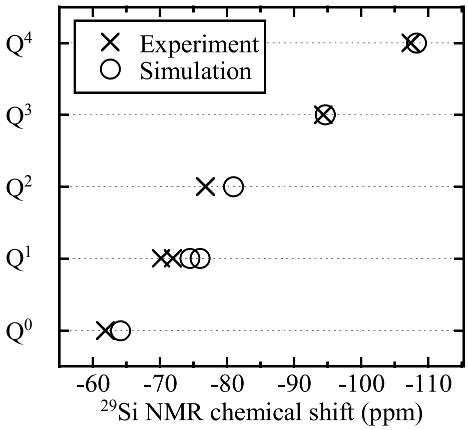

Figure 2. The ^{29}Si NMR chemical shift of Si atoms in Q^n species (Q^n are SiO_4 units containing n *bridging oxygens) in silicate crystals (Q^4 in SiO_2, Q^3 in $Na_2Si_2O_5$, Q^2 in Na_2SiO_3, Q^1 in $Ca_3Si_2O_7$, Q^0 in Mg_2SiO_4)*

stabilise the structures. In the cluster models, SiO_4 units were centrally positioned and four SiO_4, BO_4 or BO_3 units were additionally placed around the central SiO_4 unit. Q^{0-3} species including NBOs were also constructed. Sodium ions were introduced to compensate the negative charges of BO_4 units and NBOs. Hydrogen atoms were also added to the terminal oxygen atoms to reduce bond termination effects.

A cluster model of a Q^4 species surrounded by three SiO_4 units and one BO_4 unit is shown in Figure 1. Geometry optimisation was performed by using the Gaussian03 program at the HF6-31G(d) level. In the geometry optimisation, hydrogen atoms were firstly optimised, and secondly the central SiO_4 unit was fixed and the surrounding atoms, including hydrogen and alkali atoms, were optimised. Lastly the limitations were removed, and all atoms in a cluster were optimised, obtaining a final structure.

NMR parameters were obtained by making calculations with the Gaussian03 program at the HF/6-311+G(2df,p) level. Magnetic shielding parameters were calculated by using the Gauge-Independent Atomic Orbital (GIAO) method.(10) Chemical shifts, δ, for ^{29}Si NMR (in ppm) were estimated from the following equation

$$\delta(\text{cluster})=\sigma(\text{TMS})-\sigma(\text{cluster}) \qquad (1)$$

where σ is the ^{29}Si magnetic shielding (in ppm) obtained from MO calculations. Tetra methyl silane (TMS) was used as a reference. The TMS cluster geometry was optimised at the HF/6-31G(d) level, and the shielding parameter was calculated at the HF/6-311+G(2df,p) level.

Results

Firstly, Q^n structures were extracted from various silicate crystals, and the ^{29}Si NMR chemical shifts for Si atoms in each of the Q^n species were estimated for the purpose of evaluating the validity of the cluster models and the calculation conditions. As shown in Figure 2, the ^{29}Si NMR chemical shift along with the change in Q^n structure is successfully reproduced, indicating that the calculation methods used are applicable to borosilicate structures.

Figure 3 shows the ^{29}Si NMR chemical shift calculated from the borosilicate clusters $Q^4(kBm)$ (Q^4 species surrounded by k BO_m units). High frequency shift with increasing number of BO_4 units surrounding the central Q^4 species is commonly confirmed, both in the cluster models extracted from the borosilicate crystals, and the hand built clusters after geometry optimisation. The chemical shifts of the Q^4 species associated with two and three BO_4 units (k=2, 3) are slightly different, but the other Q^4 species (k=0, 1, 4) are in good agreement between the cluster models constructed in different ways. It is noted that the chemical shifts of the Q^4 species associated with more than one BO_4 unit (k=2, 3, 4) are nearly identical to

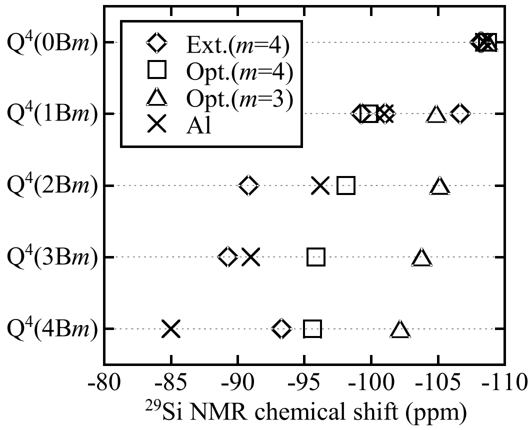

Figure 3. The ^{29}Si NMR chemical shift of Si atoms in various Q^4 species surrounded by BO_m units. Q^4(kBm) indicates Q^4 species surrounded by k *BO_m units. Ext.: cluster models extracted from borosilicate crystals (k=0: SiO_2, 1: $KNa_2B_3Si_{12}O_{30}$, $KBSi_3O_8$, $NaBSi_3O_8$, 2: $KBSi_2O_6$, 3: $CaB_2Si_2O_8$, 4: $NaBSiO_4$). Opt.: hand built cluster models after geometry optimisation. Al: experimental chemical shift of Q^4 species surrounded by AlO_4 units in aluminosilicate crystals(8)*

those of the Q^3 species in alkali silicates. Figure 3 also shows the chemical shifts of Q^4 species associated with BO_3 units (m=3). Borosilicate crystals consisting of such structures could not be found, and hence the cluster models consisting of Si–O–B3 bonds were constructed by the hand built method. As shown in Figure 3, the ^{29}Si NMR chemical shifts due to B3 coordination to an SiO_4 unit are smaller than those due to B4 coordination. It is consequently concluded that the −90 ppm component in the ^{29}Si NMR signal of borosilicate glasses can be attributed to Q^4 species associated with more than one BO_4 unit.

Discussion

Lippmaa *et al*(8) reported the ^{29}Si NMR chemical shift for various aluminosilicates. For comparison, the chemical shift of Q^4 species in aluminosilicates is also illustrated in Figure 3. A linear change in the chemical shift occurs as the number of AlO_4 units associated with the SiO_4 unit increases. It is noted that the calculated chemical shifts of the Q^4(*k*B4) species are quite similar to the experimental shifts of the Q^4(*k*Al) species, except for *k*=4. If B4 and Al coordination to SiO_4 unit actually results in a similar ^{29}Si NMR chemical shift, this seems a curious phenomenon because B and Al atoms have different size and electronegativity.

According to the simplest interpretation, the NMR chemical shift depends on the electron population of objective atoms; when the electron population at outer shells increases, the core orbitals such as Si 1s, 2s and 2p expand and increase in orbital energy. As a result, Si nuclei are less shielded, and the ^{29}Si NMR signal shifts to the higher frequency (lower magnetic field) side. Based on this interpretation, the electron population of Si atoms in Q^4 species should increase with increasing number of surrounding BO_4 or AlO_4 units. Pauling's electronegativity for B, Al and Si atoms is 2·0, 1·6 and 1·8, respectively. Therefore, it is reasonable that more electrons are populated on Si in Si–O–Al bonds, whilst less electrons are populated on Si in Si–O–B bonds. However, this is inconsistent with the ^{29}Si NMR chemical shift predicted by the MO calculations.

The electronic states of Si, such as electron population and core orbital energy, were then examined. According to Mulliken population analysis,(11) the electron population on Si is given by $Q_{Si}=Q_{SiSi}+\frac{1}{2}\Sigma Q_{SiO}$, where Q_{SiSi} and Q_{SiO} are the populations of nonbonding electrons localised on Si and electrons shared between Si and neighbouring oxygens, respectively. In this paper, the total electron population around a Si nucleus was estimated as $Q_{SiSi}+\Sigma Q_{SiO}$, without dividing the shared electrons between Si and O. As shown in Figure 4(a), a linear correlation between total electron population on Si and ^{29}Si NMR chemical shift is confirmed in the Q^n species extracted from silicate crystals. In the case of borosilicate cluster models, however, it is difficult to recognise the changes in continuous sequence in electron population. Especially, in the case of B3 coordination, the change in electron population is completely opposite. As for the Si1s orbital energy, shown in Figure 4(b), a correlation which is not linear, but has a downward sloping trend, is commonly observed even in the borosilicate cluster models, and similar correlations are also confirmed against Si2s and Si2p orbital energies. It is suggested from these results that the electron population is not the decisive factor in determining the ^{29}Si NMR chemical shift.

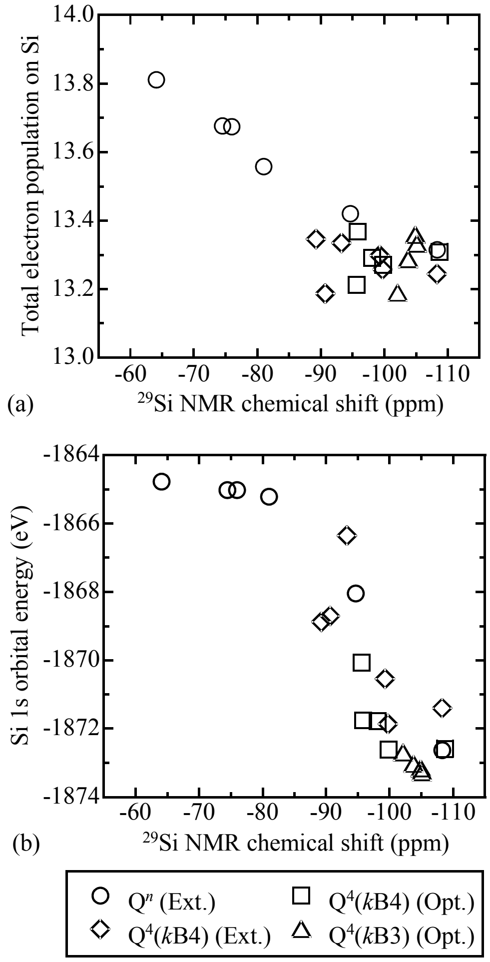

Figure 4. Correlation of the calculated ^{29}Si NMR chemical shift with (a) total electron population on the Si atom, and (b) Si1s orbital energy. Q^n (Ext.) and Q^4(kB4) (Ext.) represent the cluster models extracted from silicate crystals (see Figure 2) and borosilicate crystals (see Figure 3), respectively. Q^4(kB4) (Opt.) and Q^4(kB3) (Opt.) indicate the hand built cluster models after geometry optimisation

It is known that ^{29}Si NMR chemical shift is also dependent on bond angle, and Xue & Kanzaki(12,13) reported the angular dependence for Si–O–T bonds (T=Si, Al) by using MO calculations. Hence the angular dependence for Si–O–T bonds (T=Si, B3, B4) in borosilicate structures was also examined. Figure 5 shows the angular dependence of the ^{29}Si NMR chemical shift, where the bond angles of central Si–O bonds to the surrounding Si, B3 and B4 atoms are averaged. A good correlation is recognised between the ^{29}Si

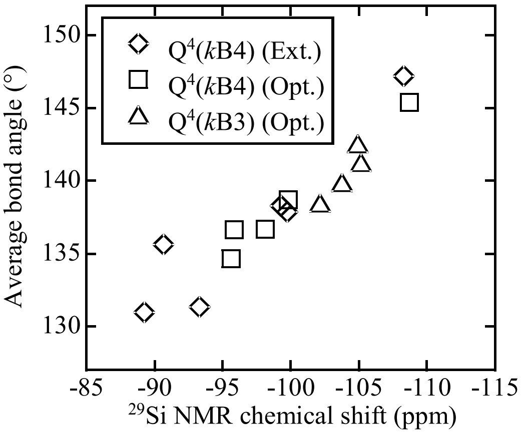

Figure 5. The correlation between the calculated ^{29}Si NMR chemical shift and the average bond angle for Si–O–(Si,B) bonds. Q^4(kB4) (Ext.) represents the cluster models extracted from borosilicate crystals (see Figure 3). Q^4(kB4) (Opt.) and Q^4(kB3) (Opt.) indicate the hand built cluster models after geometry optimisation

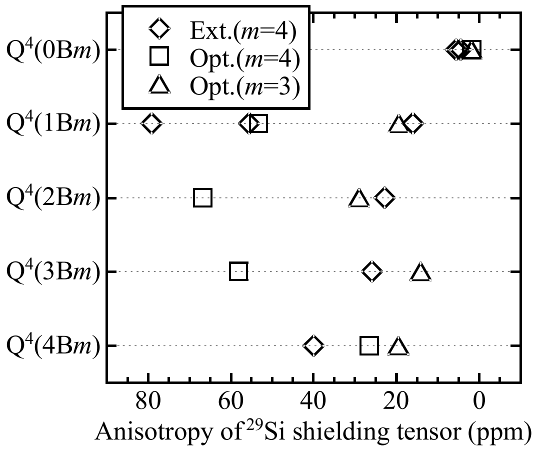

Figure 6. The anisotropy of the ^{29}Si shielding tensor of Si atoms in various Q^4 species surrounded by BO_m units, Q^4(kBm). Ext.: cluster models extracted from borosilicate crystals (see Figure 3). Opt.: hand built cluster models after geometry optimisation

NMR chemical shift and the average bond angle for the Si–O–(Si,B) bonds. It is consequently suggested that the boron coordination to SiO_4 unit results in a decrease in the Si–O–B bond angle, and hence leads to a higher frequency shift of the ^{29}Si NMR signal.

As discussed, boron coordination to SiO_4 units resulted in a change of bond angle and ^{29}Si NMR chemical shift to the higher frequency side. The change in bond angle may also induce chemical shift anisotropy, and hence the change in anisotropy of the ^{29}Si shielding tensor was investigated. As shown in Figure 6, the change in anisotropy of Si atoms in cluster models extracted from borosilicate crystals is not systematic. In the case of Si atoms in cluster models after geometry optimisation, however, maxima in anisotropy are confirmed for Si atoms surrounded by two BO_4 or BO_3 units, and larger anisotropy is caused by the coordination of BO_4 units. The anisotropy of the ^{29}Si shielding tensor of a Si atom in a cluster model of Q^3 structure after geometry optimisation is 94·6 ppm, which is much larger than that of Q^4(2B4) of 66·8 ppm. It is concluded from these results that discrimination between Si atoms in Q^3 and Q^4(*k*B4) species is almost impossible by ^{29}Si MAS NMR, but for ^{29}Si static NMR, however, it may be possible based on the asymmetric parameters of the NMR signal.

Conclusions

^{29}Si NMR chemical shifts were examined by using molecular orbital calculations. Various Q^4 structural models were constructed, changing the number of BO_m units surrounding the central SiO_4 unit, and the effect of boron coordination to SiO_4 units on the ^{29}Si NMR chemical shift was investigated. As the number of BO_4 units surrounding the central SiO_4 unit increased, chemical shifts to the higher frequency side were observed, both for cluster models extracted from borosilicate crystals, and for hand built clusters after geometry optimisation. The chemical shifts of the Q^4 species associated with more than one BO_4 unit were nearly identical to those of the Q^3 species in alkali silicates, leading to the conclusion that the –90 ppm component observed in the ^{29}Si NMR signal in borosilicate glasses may also be attributed to Q^4 species associated with more than one BO_4 unit. In the case of Q^n species in silicates, the change in the electron population on Si atoms which is caused by the formation of NBOs in SiO_4 units is the predominant factor for the ^{29}Si NMR chemical shift. In the case of Q^4 species in borosilicates, however, the change in the bond angle for Si–O–(Si,B4) bridges is the most significant factor determining the chemical shift. Discrimination between Q^3 and BO_4-associated Q^4 species seems to be impossible by using ^{29}Si MAS NMR, but these species have different anisotropy of the ^{29}Si shielding tensor, suggesting the possibility that they can be distinguished by using ^{29}Si static NMR measurements.

References

1. Dell, W. J., Bray P. J. & Xiao S. Z. *J. Non-Cryst. Solids*, 1983, **58**, 1.
2. Zhong, J., Wu, X., Liu, M. L. & Bray, P. J. *J. Non-Cryst. Solids*, 1988, **107**, 81.
3. MacKenzie, J. W., Bhatnagar, A., Bain, D., Bhowmik, S., Parameswar, C., Budhwani, K., Feller, S. A., Royle, M. L. & Martin, S. W. *J. Non-Cryst. Solids*, 1994, **177**, 269.
4. Miura, Y., Kusano, H., Nanba, T. & Matsumoto, S. *J. Non-Cryst. Solids*, 2001, **290**, 1.
5. Nanba, T. & Miura, Y. *Phys. Chem. Glasses*, 2003, **44**, 244.
6. Nanba, T., Nishimura, M. & Miura, Y. *Geochim. Cosmochim. Ac.*, 2004, **68**, 5103.
7. Maekawa, H., Maekawa, T., Kawamura, K. & Yokokawa, T. *J. Non-Cryst. Solids*, 1991, **127**, 53.
8. Lippmaa, E., Maegi, M., Samoson, A., Tarmak, M. & Engelhardt, G. *J. Am. Chem. Soc.*, 1981, **103**, 4992.
9. GAUSSIAN 03, Gaussian, Inc., Pittsburgh, PA, 2003.
10. Cheeseman, J. R., Trucks, G. W., Keith, T. A. & Frisch, M. J. *J. Chem. Phys.*, 1996, **104**, 5497.
11. Mulliken R. S. *J. Chem. Phys.*, 1955, **23**, 1833.
12. Xue, X. & Kanzaki, M. *Phys. Chem. Miner.*, 1998, **26**, 14.
13. Xue, X. & Kanzaki, M. *J. Phys. Chem. B*, 1999, **103**, 10816.